Measurement of Two-Dimensional Energy Spectra in a Turbulent Boundary Layer

D. Chandran, R. Baidya, J. P. Monty and I. Marusic

Department of Mechanical Engineering
The University of Melbourne, Victoria 3010, Australia

Abstract

Here we present an experimental technique using hot-wire anemometry to measure the two-dimensional (2-D) energy spectra of the streamwise velocity component (u). The measurements are carried out in a turbulent boundary layer at friction Reynolds numbers of 1950 and 3350 and are validated against the 2-D spectra obtained from the direct numerical simulation (DNS) of Sillero et al. [9] at matched Reynolds numbers. Based on these comparisons, a correction is introduced to account for the spatial resolution associated with the initial separation of the hot-wires. These findings establish the proposed technique for high Reynolds number flows in future works.

Introduction

Spectral scaling laws are important in turbulent boundary layer studies as they provide information regarding the geometry of turbulent structures and their contribution to the turbulent kinetic energy. Among them, k_x^{-1} scaling of one-dimensional (1-D) streamwise spectra of u in the inertial region of turbulent boundary layer is of specific interest as it indicates the wall scaling of turbulent structures. Here, k_x is the streamwise wavenumber. Previously, theoretical predictions of k_x^{-1} scaling were based on dimensional analysis [6] and spectral overlap arguments [7]. These findings were also found to be consistent with the attached eddy hypothesis of Townsend [10], which predicts the existence of geometrically self-similar eddies. Consequently, a range of length scales exist that contribute equally to the turbulent kinetic energy and thereby results in a k_x^{-1} behaviour in the 1-D streamwise spectra at sufficiently high Reynolds numbers. Nevertheless, these predictions did not get complete support from high Reynolds number experiments and the existence of a k_x^{-1} law still remains an open question [5, 8].

Davidson et al. [2] highlighted that the 1-D energy spectra might not be an ideal tool to observe self-similarity. Their work suggested that aliasing could contaminate the 1-D streamwise spectra by artificially shifting the energy to lower wavenumbers. Whereas, a 2-D spectrum details the contribution of both the streamwise ($\lambda_x = 2\pi/k_x$) and spanwise ($\lambda_y = 2\pi/k_y$, where k_y is the spanwise wavenumber) length scales to the total turbulent intensity. On the other hand, a 1-D spectrum is a line integral of a 2-D spectra and does not reveal any information along the direction of integration. For example, a 1-D streamwise spectrum only provides the energy contribution by a particular streamwise length scale, λ_x, and does not inform us of the range of λ_y associated with that particular λ_x. This leads to the aforementioned aliasing in 1-D spectra. The 2-D spectrum is devoid of such aliasing errors.

From dimensional considerations, Chung et al. [1] argued that, in order to have a k_x^{-1} behaviour in the 1-D spectrum, a region of constant energy in the 2-D spectrum should be bounded by $\lambda_y/z \sim f_1(\lambda_x/z)$ and $\lambda_y/z \sim f_2(\lambda_x/z)$ where f_1 and f_2 are identical power laws. At low Reynolds number,

Del Alamo et al. [3] reported that such a region of constant energy is bounded at larger scales by a square-root relationship of the form $\lambda_y/z \sim (\lambda_x/z)^{1/2}$. However, on the basis of attached eddy hypothesis, the existence of geometrically self-similar eddies (whose lengths scale with z) suggest such a region at high Reynolds numbers to be bounded by a linear relationship, $\lambda_y \sim \lambda_x$. However, to discern such a behaviour, 2-D spectra at high Reynolds numbers need to be examined. As a first step towards high Reynolds number results, this paper is concerned with establishing a reliable experimental technique to measure 2-D spectra of u. Validation of the experimental results with required corrections to obtain a well resolved 2-D spectra is described in the following sections.

It should be noted that, throughout this study, x, y and z denotes the streamwise, spanwise and wall-normal directions respectively and u, v and w denotes the corresponding velocity components. Superscript '+' indicates the normalisation using viscous length and velocity scales which are ν/U_τ and U_τ respectively, where ν is the kinematic viscosity and U_τ is the friction velocity.

Experimental Setup

The experiments are conducted in the open return turbulent boundary layer wind tunnel at The University of Melbourne. The facility is a zero pressure gradient (ZPG) tunnel with a test section volume of $6.7 \times 0.94 \times 0.38$ m^3. The experiments are all conducted at a streamwise location of $x = 3.8$ m, further details are provided in table 1. Here we define the boundary layer thickness, δ as the wall-normal distance where the mean velocity achieves 99 % of the freestream velocity. Further, the friction velocity, U_τ, is obtained by a Clauser chart method using the log law constants, $\kappa = 0.4$ and A$= 5$.

The tailored experimental technique uses two single-wire hot-wire probes: HW1 and HW2 (as shown in figure 1). The length (l) and diameter (d) of the hot-wire sensors are 500μm and 2.5μm respectively to maintain an l/d ratio of 200 and $l^+ \approx 17$. The hot-wires, operated using an in-house Melbourne University constant temperature anemometer (MUCTA), are sampled at 30kHz for $T = 120$ seconds. This corresponds to about 32000 and 49000 boundary layer turnover time (TU_∞/δ) for $Re_\tau = 1950$ and 3350 respectively. Both hot-wires are calibrated immediately before and after each measurement. This allows us to account for any drift in the hot-wire voltage during the measurements. HW1 is calibrated in the freestream with respect to the known mean velocities obtained with a Pitot-static probe. Since the arrangement did not allow HW2

U_∞ (m/s)	δ (m)	U_τ (m/s)	Re_τ	z^+
15	0.056	0.545	1950	100
15	0.056	0.545	1950	200
25	0.061	0.86	3350	200

Table 1: Details of experimental data.

to move to the freestream, calibration information from HW1 is used to calibrate HW2, while placed inside the boundary layer. This is achieved by placing both wires at the same wall-normal location. Since this calibration is carried out inside the turbulent boundary layer, the sampling time is increased compared to the freestream calibrations to ensure the convergence of mean velocity.

At the start of the measurement, HW1 and HW2 are positioned close to each other, at a fixed wall-normal location, as shown in figure 1. $dy_{initial}$ corresponds to the initial centre to centre spacing between the hot-wire sensors. For the present measurements, both HW1 and HW2 are sampled simultaneously, with HW1 at a fixed position, while HW2 is traversed in the spanwise direction upto a final spacing of $\Delta y \sim 3.5\delta$ (see figure 1). To acquire spatial information at smaller spanwise distances the spanwise traversing mechanism of HW2 is traversed on a logarithmic scale.
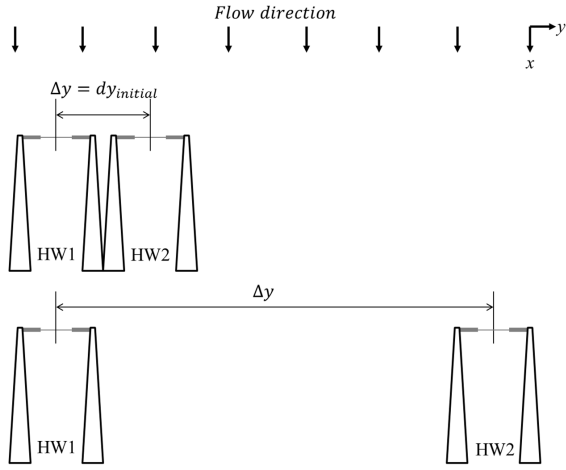
Figure 1: Schematic of the arrangement of hot-wires to measure the spanwise correlation.

Calculation of 2-D Spectra

In the present work, the streamwise velocity fluctuations, u_1 and u_2, acquired simultaneously using HW1 and HW2 respectively (for different spanwise spacings (Δy)) are used to construct the 2-D correlation and thus the 2-D energy spectra of u. To this end, HW2 is physically traversed to construct the correlation in the spanwise direction. Thereafter, the use of Taylor's frozen turbulence hypothesis allows the construction of correlation functions at different streamwise spacings (Δx). We note, since the hot-wires (HW1 and HW2) are stationed at the same wall-normal location, spanwise homogeneity within the turbulent boundary layer can be assumed. As a consequence, the entire spanwise correlation can be constructed from a series of independent two-point measurements conducted at different Δy. Hence, a 2-D correlation can be constructed by cross-correlating the streamwise velocity time series acquired using HW1 and HW2 by computing,

$$R_{uu}(\Delta x, \Delta y) = \overline{u_1(x,y) u_2(x+\Delta x, y+\Delta y)}. \quad (1)$$

Figure 2(a) shows the 2-D correlation obtained along with the projections of 1-D correlations. The black and red contours correspond to the 1-D streamwise and spanwise correlations respectively. Here, R_{uu} is normalised using the variance of the velocity time series to get $\mathcal{R}_{uu}$. Figure 2(b) shows the 2-D energy
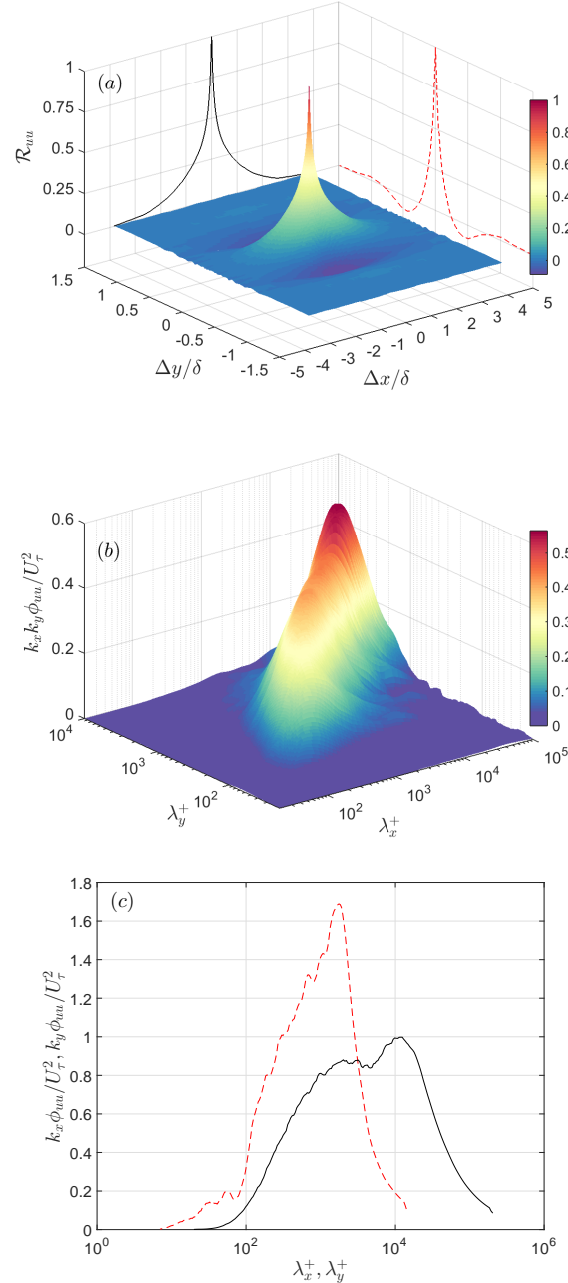
Figure 2: (a) Normalised 2-D correlation constructed from the velocity time series with projections of 1-D correlations at $\Delta x = 0$ and $\Delta y = 0$, (b) 2-D spectra obtained from the 2-D correlation and (c) 1-D streamwise (—) and 1-D spanwise (- - -) spectra obtained by integrating the 2-D spectra.

spectrum of streamwise velocity fluctuations which is obtained by taking a two dimensional Fourier transform of $R_{uu}(\Delta x, \Delta y)$,

$$\phi_{uu}(k_x, k_y) = \int\int_{-\infty}^{\infty} R_{uu}(\Delta x, \Delta y) e^{-j2\pi(k_x\Delta x + k_y\Delta y)} \mathrm{d}(\Delta x)\mathrm{d}(\Delta y). \quad (2)$$

Here j is a unit imaginary number. Results for $\phi_{uu}(k_x, k_y)$ are presented as a function of λ_x and λ_y. If one considers the streamwise (λ_x) and spanwise (λ_y) length scales as the length and width (respectively) of the eddies in the flow, the 2-D spectrum can be considered as energy contribution of different as-

pect ratio eddies. Figure 2(c) shows the 1-D streamwise and spanwise spectra of u obtained after integrating the 2-D spectrum (shown in figure 2(b)) across λ_y and λ_x respectively. We note that the area under the 1-D streamwise and spanwise spectra is equivalent to the variance of the streamwise velocity at that wall-normal location.

Validation & Correction using DNS

The results obtained from the experiments are validated against the DNS of ZPG boundary layer data of Sillero *et al.* [9]. To this end, a two-dimensional Fourier transformation is carried out on the 2-D correlation obtained from the DNS database. Figure 3 shows a comparison between a contour of constant energy from the 2-D spectra, at $k_x k_y \phi_{uu}/U_\tau^2 = 0.15$, from both experiments and DNS. The results show good agreement between the experimental ($\cdots$) and DNS (—) results at $z^+ \approx 200$ (figure 3b), however, closer to the wall ($z^+ \approx 100$) a larger disagreement in the small scale region is present (figure 3a). This discrepancy is likely to be caused by insufficient spatial resolution of the experiments due to the initial spacing ($dy_{initial}$) between the hot-wires (see figure 1). It is to be noted that the spatial resolution issue dealt with in this study is related to the initial spacing between the hot-wires ($dy_{initial}^+$) and not to the sensor size (l^+). From figure 1, the smallest spanwise length scale that can be resolved by this arrangement of hot-wires is limited to $dy_{initial}$. Therefore, all the points between $\Delta y = 0$ and $\Delta y = dy_{initial}$ in the spanwise correlation map are obtained by linear interpolation (other interpolation schemes were found to be more susceptible to noise present in the experimental data). Hence, the wavelength corresponding to a spanwise spacing of $dy_{initial}^+$ would act as a cut-off wavelength (dashed line in figure 3) and all the smaller scales (below the dashed line) could be impacted by the uncertainty of the interpolation scheme. We note that this discrepancy is more significant closer to the wall as there is more contribution from scales closer to the cut-off wavelength (at $z^+ \approx 100$). Further, the area under the 2-D spectra has to be equal to the variance at that wall-normal location, therefore, any unresolved energy at smaller scales would be redistributed across larger scales. Hence, to minimise such a scenario, ideally $dy_{initial}^+$ should be sufficiently smaller so that the smallest scales are well resolved. However, for the present experimental technique, it is not physically possible to reduce $dy_{initial}^+$ below a limit where the two hot-wires come in contact with each other. This calls for the necessity of a correction scheme to account for the spatial resolution issue associated with the initial spacing between the hot-wires.

Accordingly, a method is adopted based on the DNS data available, to correct for the spatial resolution issue associated with
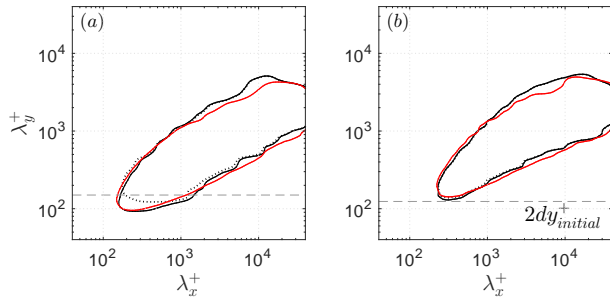
$dy_{initial}^+$. Figure 4 shows the 1-D correlation in the spanwise direction obtained using DNS data, which is interpolated to match the experimental resolution. Here, the data points corresponding to a spanwise length of $\Delta y^+ \leq dy_{initial}^+$ is initially omitted from the original correlation but is recomputed using linear interpolation scheme (red symbols in figure 4) to match the experimental conditions. The computed 2-D spectra from the original and interpolated DNS correlation functions are shown in figures 5(a) and 5(b) respectively. The difference ($\Delta k_x k_y \phi_{uu}^+$) of the two spectra is computed and shown in figure 5(c). This difference corresponds to the amount of energy redistributed due to $dy_{initial}^+$. The 2-D spectra calculated from experiments is now corrected by adding this difference to it. Namely,

$$\Delta k_x k_y \phi_{uu}^+ = \left[\frac{k_x k_y \phi_{uu}}{U_\tau^2} \right]_{DNS,o} - \left[\frac{k_x k_y \phi_{uu}}{U_\tau^2} \right]_{DNS,i} \quad (3)$$

$$\left[\frac{k_x k_y \phi_{uu}}{U_\tau^2} \right]_{EXP,c} = \left[\frac{k_x k_y \phi_{uu}}{U_\tau^2} \right]_{EXP} + \Delta k_x k_y \phi_{uu}^+. \quad (4)$$

where the subscripts DNS,o and DNS,i represents original and interpolated DNS results respectively. Similarly, EXP,c and EXP represents the corrected and uncorrected experimental results respectively. As one would expect, the difference is largest near λ_y^+ corresponding to $dy_{initial}^+$ (see white dashed line in figure 5). A contour of constant energy in the corrected experimental spectrum (—) is compared against the DNS(—) as shown in figure 3. A good agreement with DNS is observed at smaller scales where as the uncorrected experimental spectrum ($\cdots$) shows a mismatch.

Relevance to High Reynolds number Measurements

The present work is aimed to set the stage for a larger experimental campaign at higher Reynolds numbers. To this end, the correction method discussed is highly relevant as the smallest scales are typically harder to resolve with increasing Reynolds numbers. Consequently, one would require even smaller spacing between the hot-wires to maintain a fixed spacing in viscous units. Hutchins *et al.* [4] has shown that at smaller scales, the energy contribution shows minimal variance with increasing Reynolds numbers. Equipped with this knowledge, the proposed correction scheme can be easily applied to high Reynolds number databases as well. To illustrate this, the DNS data obtained at $Re_\tau \approx 2000$ is used to correct the experimental data obtained at $Re_\tau = 3350$ at matched z^+. The results are given in figure 6 which show good agreement at the smaller scales between the uncorrected experimental and interpolated DNS spectrum (figure 6a). Furthermore, after the correction, the small

Figure 3: Comparison of experimental and DNS results for $k_x k_y \phi_{uu}/U_\tau^2 = 0.15$ at $Re_\tau \approx 2000$ and, (a) $z^+ \approx 100$ and (b) $z^+ \approx 200$; where, $\cdots\cdots$ uncorrected experiment; —— corrected experiment and —— DNS
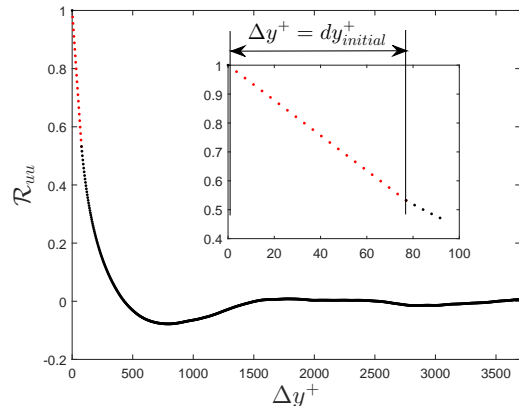
Figure 4: 1-D spanwise correlation demonstrating the method of correcting $dy_{initial}^+$ error.
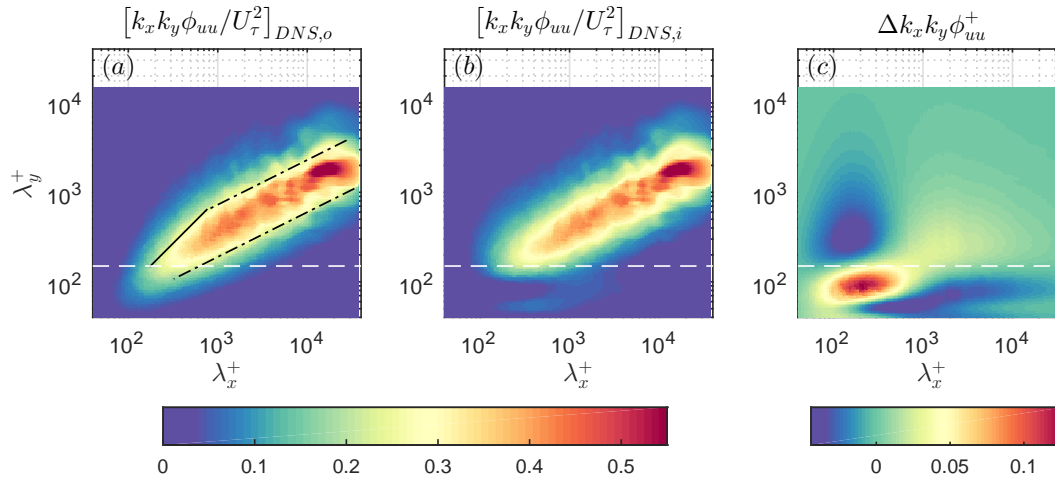
Figure 5: (a) 2-D spectra obtained from the original DNS correlation, where ——— and - - - represent the relationships $\lambda_y/z \sim \lambda_x/z$ and $\lambda_y/z \sim (\lambda_x/z)^{1/2}$ respectively as reported by Del Alamo *et al.* [3], (b) 2-D spectra obtained from the interpolated DNS correlation and (c) difference between (a) and (b).
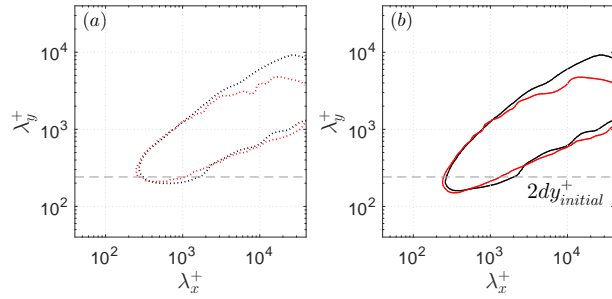
Figure 6: Comparison of experimental ($Re_\tau = 3350$) and DNS ($Re_\tau \approx 2000$) results at $k_x k_y \phi_{uu}/U_\tau^2 = 0.15$, (a) before correction where, ······ uncorrected experiment and ······ interpolated DNS and (b) after correction where, ——— corrected experiment and ——— original DNS

scales now agree with the original DNS 2-D spectrum (figure 6b). The agreement is only expected at smaller scales since we are comparing two different Reynolds numbers. Therefore, the proposed correction enables one to compare the 2-D spectra across multiple Reynolds numbers and wall heights, while still maintaining a practical $dy_{initial}$.

Summary and Conclusions

An experimental technique to measure the 2-D energy spectra of the streamwise velocity in a turbulent boundary layer is introduced. The technique involves the use of a pair of hot-wire sensors that are sampled simultaneously for different spanwise spacings. A description of how to construct a 2-D correlation, as a function of streamwise and spanwise distance, from the velocity time series is presented. This procedure is then used to compute the 2-D spectra, as a function of streamwise and spanwise wavelengths. Results are validated against the statistics computed from DNS databases at matched Reynolds numbers. This comparison revealed the importance of the initial spacing between the hot-wires and its detrimental impact on resolving the small scale region of the 2-D spectra. To account for this, a correction scheme is outlined based on results computed from DNS databases. Collectively, the proposed experimental technique and correction schemes lay a foundation for future works at higher Reynolds numbers.

References

[1] Chung, D., Marusic, I., Monty, J.P., Vallikivi, M., and Smits, A.J., On the universality of inertial energy in the log layer of turbulent boundary layer and pipe flows, *Exp. Fluids*, **56**, 2015, 1–10.

[2] Davidson, P.A., Nickels, T.B. and Krogstad, P-A., The logarithmic structure function law in wall-layer turbulence, *J. Fluid. Mech*, **550**, 2006, 51–60.

[3] Del Alamo, J.C., Jimenez, J., Zandonade, P. and Moser, R.D., Scaling of the energy spectra of turbulent channels, *J. Fluid. Mech*, **500**, 2004, 135–144.

[4] Hutchins, N., Nickels, T.B, Marusic, I. and Chong, M.S., Hot-wire spatial resolution issues in wall-bounded turbulence, *J. Fluid. Mech*, **635**, 2009, 103–136.

[5] Nickels, T.B., Marusic, I., Hafez, S. and Chong, M.S., Evidence of the k_1^{-1} law in a high-Reynolds-number turbulent boundary layer, *Phys. Rev. Lett*, **95**, 2005, 074501.

[6] Perry, A.E. and Chong, M.S., On the mechanism of wall turbulence, *J. Fluid. Mech*, **119**, 1982, 173–217.

[7] Perry, A.E., Henbest, S. and Chong, M.S., A theoretical and experimental study of wall turbulence, *J. Fluid. Mech*, **165**, 1986, 163–199.

[8] Rosenberg, B.J., Hultmark, M., Vallikivi, M., Bailey, S.C.C. and Smits, A.J., Turbulence spectra in smooth and rough-wall pipe flow at extreme Reynolds numbers, *J. Fluid. Mech*, **731**, 2013, 46–63.

[9] Sillero, J.A., Jimenez, J. and Moser, R.D., Two-point statistics for turbulent boundary layers and channels at Reynolds numbers up to $\delta^+ \approx 2000$, *Phys. Fluids*, **26**, 2014, 105109.

[10] Townsend, A.A., *The structure of turbulent shear flow*, Cambridge University Press, 1976.